Differential Effects of Cholesterol and its Immediate Biosynthetic Precursors on Membrane Organization[†]

Sandeep Shrivastava, Yamuna Devi Paila, Aritri Dutta, and Amitabha Chattopadhyay*

Centre for Cellular and Molecular Biology, Uppal Road, Hyderabad 500 007, India

Received January 29, 2008; Revised Manuscript Received February 26, 2008

ABSTRACT: Cholesterol is the most representative sterol present in vertebrate membranes and is the end product of the long and multistep sterol biosynthetic pathway. 7-Dehydrocholesterol (7-DHC) and desmosterol are the immediate biosynthetic precursors of cholesterol in the Kandutsch-Russell and Bloch pathway. In this article, we have monitored the effect of cholesterol and its two immediate biosynthetic precursors on biophysical and dynamic properties of fluid and gel phase membranes. Toward this goal, we have used fluorescent membrane probes, DPH and TMA-DPH, and the hydrophobic probe, pyrene. Our results using these probes show that although both 7-DHC and desmosterol differ with cholesterol in one double bond, they exhibit differential effects on membrane organization and dynamics. Importantly, we show that the effect of cholesterol and desmosterol on membrane organization and dynamics is similar in most cases, while 7-DHC has a considerably different effect. This demonstrates that the position of the double bond in sterols is an important determinant in maintaining membrane order and dynamics. These results assume relevance since the accumulation of cholesterol precursors have been reported to result in severe pathological conditions.

Cholesterol is an essential constituent of eukaryotic membranes and plays a crucial role in membrane organization, dynamics, function, and sorting (*1, 2*). It is often found distributed nonrandomly in domains or pools in biological and model membranes and is thought to contribute to a segregated distribution of membrane constituents (*1–3*). Cholesterol is proposed to maintain a laterally heterogeneous distribution of lipids and proteins on the plasma membrane because of its putative role in inducing domains such as lipid rafts (*4*). Many of these domains are believed to be important for the maintenance of membrane structure and function. Such membrane domains have been implicated in important cellular functions such as signal transduction (*5*) and entry of pathogens into the cell (*6*).

Cholesterol is the most representative sterol present in vertebrate membranes and is the end product of the long and multistep sterol biosynthetic pathway. There are two major pathways for cholesterol biosynthesis, the Kandutsch-Russell (*7*) and Bloch (*8*) pathways. Konrad Bloch speculated that the sterol biosynthetic pathway parallels sterol evolution (the Bloch hypothesis). According to this hypothesis, cholesterol has been selected over a very long time scale of natural evolution for its ability to optimize certain physical properties of eukaryotic cell membranes with regard to biological functions (*8*). Cholesterol precursors should therefore have properties that gradually support the cellular function of higher organisms as they progress along the pathway toward cholesterol. Defects in the cholesterol biosynthetic pathway have been identified with several inherited metabolic disorders (*9*). Comparative studies of the effects of cholesterol and its evolutionary precursors on membranes therefore assume significance.

7-Dehydrocholesterol (7-DHC[1]) is an immediate biosynthetic precursor of cholesterol in the Kandutsch-Russell pathway and is reduced to cholesterol in the final step by the enzyme 3β-hydroxy-steroid-Δ^7-reductase (7-DHCR). 7-DHC differs with cholesterol only in a double bond at the 7th position in the sterol ring (see Figure 1) (*10*). Desmosterol is the immediate biosynthetic precursor of cholesterol in the Bloch pathway and differs with cholesterol only in a double bond at the 24th position in the flexible alkyl side chain (Figure 1). Desmosterol is converted to cholesterol in the final step of the pathway by the enzyme 3β-hydroxy-steroid-Δ^{24}-reductase (24-DHCR). Interestingly, it has been recently reported that mice lacking cholesterol (strictly speaking, a low cholesterol, high desmosterol *Dhcr24*$^{-/-}$ knockout mouse model) are viable and exhibit a mild phenotype (they are smaller in size and are sterile) (*11*). These results are somewhat surprising since it is believed that cholesterol is an exceedingly fine-tuned molecule, perfected over millions of years of evolution, in order to optimize its biological

[†] This work was supported by research grants from the Council of Scientific and Industrial Research, Govt. of India, to A.C. Y.D.P. thanks the Council of Scientific and Industrial Research for the award of a Senior Research Fellowship. A.D. was awarded a Summer Training Program Internship by the Centre for Cellular and Molecular Biology, Hyderabad. A.C. is an Honorary Professor of the Jawaharlal Nehru Centre for Advanced Scientific Research, Bangalore, India.

* To whom correspondence should be addressed. Tel: +91-40-2719-2578. Fax: +91-40-2716-0311. E-mail: amit@ccmb.res.in.

[1] Abbreviations: 7-DHC, 7-dehydrocholesterol; 7-DHCR, 3β-hydroxy-steroid-Δ^7-reductase; 24-DHCR, 3β-hydroxy-steroid-Δ^{24}-reductase; DMPC, 1,2-dimyristoyl-*sn*-glycero-3-phosphocholine; DPH, 1,6-diphenyl-1,3,5-hexatriene; DPPC, 1,2-dipalmitoyl-*sn*-glycero-3-phosphocholine; LUV, large unilamellar vesicle; POPC, 1-palmitoyl-2-oleoyl-*sn*-glycero-3-phosphocholine; SLOS, Smith−Lemli−Opitz syndrome; TMA-DPH, 1-[4-(trimethylammonio)phenyl]-6-phenyl-1,3,5-hexatriene.

10.1021/bi8001677 CCC: $40.75
Published on Web 04/29/2008

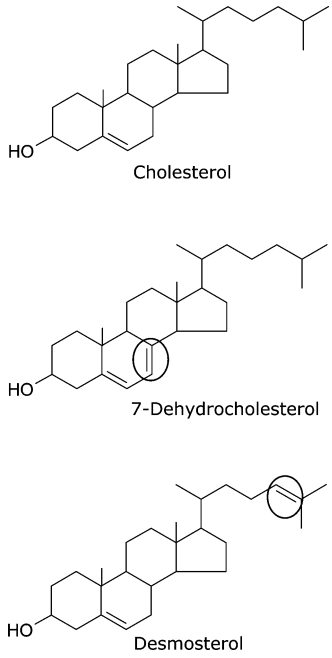

FIGURE 1: Chemical structures of the sterols used. 7-Dehydrocholesterol and desmosterol are immediate biosynthetic precursors of cholesterol in the Kandutsch-Russell (*7*) and Bloch (*8*) pathways, respectively. 7-Dehydrocholesterol differs with cholesterol only in a double bond at the 7th position in the sterol ring, and desmosterol differs with cholesterol only in a double bond at the 24th position in the flexible alkyl side chain (highlighted in their chemical structures).

function. Previous studies have shown that structural features, such as an intact alicyclic chain, a free 3β-OH group, a planar $\Delta^{5(6)}$ double bond, angular methyl groups, and a branched 7-carbon alkyl chain at the 17β-position, have all been found to be necessary for the complex biological function displayed by cholesterol (*12–15*). Close structural analogues of cholesterol, such as ergosterol, are known to give rise to membrane properties that are markedly different from those observed in membranes containing cholesterol (*16, 17*). A consequence of this fact is that the function of membrane proteins, supported by cholesterol, is often not maintained even with close analogues of cholesterol. For example, sterols that differ from cholesterol only in a double bond have been shown to exhibit different lateral pressure profiles (*18*) and are not able to support the function of membrane receptors that require cholesterol (*19, 20*). In addition, it has been reported that the activity of inward-rectifier K^+ channels is modulated even by optical isomers of cholesterol, thereby exemplifying the specificity of interaction (*21*).

Keeping in mind the importance of comparative studies of the effects of cholesterol and its precursors on membrane properties, in this work, we have monitored the effect of cholesterol and its two immediate biosynthetic precursors (7-DHC and desmosterol) on the biophysical and dynamic properties of fluid (POPC) and gel (DPPC) phase membranes. For this, we have used fluorescent membrane probes, DPH and TMA-DPH, and the hydrophobic probe, pyrene. Our results using these probes show that although both 7-DHC and desmosterol differ with cholesterol in a double bond, they exhibit differential effects on membrane organization and dynamics.

EXPERIMENTAL PROCEDURES

Materials. 1,2-Dimyristoyl-*sn*-glycero-3-phosphocholine (DMPC), cholesterol, 7-dehydrocholesterol (7-DHC), desmosterol, and pyrene were obtained from Sigma Chemical Co. (St. Louis, MO). 1,2-Dipalmitoyl-*sn*-glycero-3-phosphocholine (DPPC) and 1-palmitoyl-2-oleoyl-*sn*-glycero-3-phosphocholine (POPC) were purchased from Avanti Polar Lipids (Alabaster, AL). 1,6-Diphenyl-1,3,5-hexatriene (DPH) and 1-[4-(trimethylammonio)phenyl]-6-phenyl-1,3,5-hexatriene (TMA-DPH) were from Molecular Probes (Eugene, OR). Lipids were checked for purity by thin layer chromatography on silica gel precoated plates (Sigma) in chloroform/methanol/water (65:35:5, v/v/v) and were found to give only one spot in all cases with a phosphate-sensitive spray and on subsequent charring (*22*). The concentration of DPPC and POPC was determined by phosphate assay subsequent to total digestion by perchloric acid (*23*). DMPC was used as an internal standard to assess lipid digestion. The concentration of the stock solution of DPH, TMA-DPH, and pyrene in methanol was estimated from their respective molar absorption coefficients (ε) of 88,000 M^{-1} cm^{-1} at 350 nm for DPH and TMA-DPH and 54,000 M^{-1} cm^{-1} at 335 nm for pyrene. All other chemicals used were of the highest purity available. The solvents used were of spectroscopic grade. Water was purified through a Millipore (Bedford, MA) Milli-Q system and used throughout.

Sample Preparation. All experiments were done using large unilamellar vesicles (LUVs) of 100 nm diameter of either POPC or DPPC containing increasing concentrations (0–50 mol %) of a given sterol (cholesterol or 7-DHC or desmosterol) and 1 mol % fluorescent probe (DPH, TMA-DPH, or pyrene). In general, 640 nmol of total lipid (phospholipid and sterol) and 6.4 nmol of fluorescent probe were mixed well and dried under a stream of nitrogen while being warmed gently (~35 °C). After further drying under a high vacuum for at least 3 h, the lipid mixture was hydrated (swelled) by adding 1.5 mL of 10 mM sodium phosphate, 150 mM sodium chloride at pH 7.4 buffer, and each sample was vortexed for 3 min to uniformly disperse the lipids and form homogeneous multilamellar vesicles. The buffer was always maintained at a temperature well above the phase transition temperature of the phospholipid used as the vesicles were made. The lipids were therefore swelled at a temperature of 40 °C for POPC and 60 °C for DPPC samples. LUVs of 100 nm diameter were prepared by the extrusion technique using an Avestin Liposofast Extruder (Ottawa, Ontario, Canada) as previously described (*24*). Briefly, the multilamellar vesicles were freeze–thawed five times using liquid nitrogen to ensure solute equilibration between trapped and bulk solutions, and then extruded through polycarbonate filters (pore diameter of 100 nm) mounted in the extruder fitted with Hamilton syringes (Hamilton Company, Reno, NV). The samples were subjected to 11 passes through polycarbonate filters to give the final LUV suspension. Background samples were prepared the same way except that the fluorescent probe was not added to them. The optical density of the samples measured at 358 nm was less than 0.15 in all cases, which rules out any possibility of scattering artifacts in the anisotropy measurements. Samples were incubated in the dark for 12 h at room temperature (~23 °C) for equilibration before measuring fluorescence. All

experiments were done with multiple sets of samples at room temperature (~23 °C).

Steady State Fluorescence Measurements. Steady state fluorescence anisotropy measurements were performed with a Hitachi F-4010 spectrofluorometer using a Hitachi polarization accessory. Quartz cuvettes with a path length of 1 cm were used. For monitoring DPH and TMA-DPH fluorescence, the excitation wavelength was set at 358 nm, and emission was monitored at 430 nm. Excitation and emission slits with bandpasses of 1.5 and 10 nm were used for all measurements. The excitation slit used was the minimum possible to minimize any photoisomerization of DPH and TMA-DPH during irradiation. Fluorescence was measured with a 30 s interval between successive openings of the excitation shutter to reverse any photoisomerization of DPH and TMA-DPH (*25*). Anisotropy values were calculated from the following equation (*26*):

$$r = \frac{I_{VV} - GI_{VH}}{I_{VV} + 2GI_{VH}} \quad (1)$$

where I_{VV} and I_{VH} are the measured fluorescence intensities (after appropriate background correction) with the excitation polarizer oriented vertically and the emission polarizer vertically and horizontally oriented, respectively. G is the grating factor and is the ratio of the efficiencies of the detection system for vertically and horizontally polarized light, and is equal to I_{HV}/I_{HH}. All experiments were done with multiple sets of samples, and average values of anisotropy are shown in Figures 2 and 3.

For measuring pyrene fluorescence, samples were excited at 335 nm. Excitation and emission slits were set at 5 nm. The excimer to monomer fluorescence intensity ratio was determined by measuring fluorescence intensity at the monomer (393 nm) and excimer (480 nm) peaks. The ratio of the first (373 nm) and third (384 nm) vibronic peak intensities (I_1/I_3) was monitored from pyrene emission spectra.

Time-Resolved Fluorescence Measurements. Fluorescence lifetimes were calculated from time-resolved fluorescence intensity decays using IBH 5000F coaxial nanosecond flashlamp equipment (Horiba Jobin Yvon, Edison, NJ) with DataStation software in the time-correlated single photon counting mode. This machine uses a thyratron-gated nanosecond flash lamp filled with nitrogen as the plasma gas (~1 bar) and is run at 40 kHz. Lamp profiles were measured at the excitation wavelength using Ludox (colloidal silica) as the scatterer. To optimize the signal-to-noise ratio, 5000 photon counts were collected in the peak channel. All experiments were performed using excitation and emission slits with a bandpass of 4 nm. The sample and the scatterer were alternated after every 10% acquisition to ensure compensation for shape and timing drifts occurring during the period of data collection. This arrangement also prevents any prolonged exposure of the sample to the excitation beam, thereby avoiding any possible photodamage of the fluorophore. The data was stored and analyzed using DAS 6.2 software (Horiba Jobin Yvon, Edison, NJ). Fluorescence intensity decay curves so obtained were deconvoluted with the instrument response function and analyzed as a sum of exponential terms:

$$F(t) = \sum_i \alpha_i \exp(-t/\tau_i) \quad (2)$$

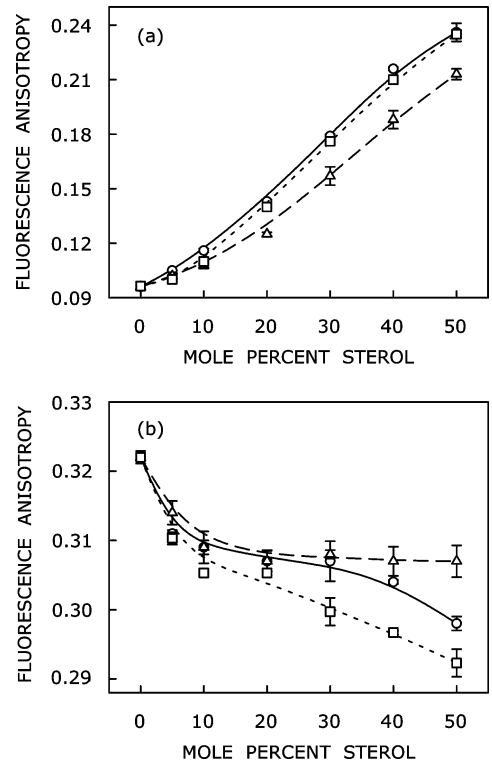

FIGURE 2: Fluorescence anisotropy of DPH in (a) POPC and (b) DPPC membranes as a function of increasing concentration of cholesterol (○, —), 7-DHC (△, — —) and desmosterol (□, ---). The ratio of DPH to total lipid was 1:100 (mol/mol), and total lipid concentration was 0.43 mM in all cases. The excitation wavelength used was 358 nm, and emission was monitored at 430 nm. Measurements were carried out at room temperature (~23 °C). Data points shown are the means ± SE of at least three independent measurements. The lines joining the data points are provided merely as viewing guides. See Experimental Procedures for other details.

where $F(t)$ is the fluorescence intensity at time t, and α_i is a pre-exponential factor representing the fractional contribution to the time-resolved decay of the component with a lifetime τ_i such that $\Sigma_i\alpha_i = 1$. The program also includes statistical and plotting subroutine packages (*27*). The goodness of the fit of a given set of observed data and the chosen function was evaluated by the χ^2 ratio, the weighted residuals (*28*), and the autocorrelation function of the weighted residuals (*29*). A fit was considered acceptable when plots of the weighted residuals and the autocorrelation function showed random deviation about zero with a minimum χ^2 value not more than 1.4. Intensity-averaged mean lifetimes $\langle\tau\rangle$ for biexponential decays of fluorescence were calculated from the decay times and pre-exponential factors using the following equation (*26*):

$$\langle\tau\rangle = \frac{\alpha_1\tau_1^2 + \alpha_2\tau_2^2}{\alpha_1\tau_1 + \alpha_2\tau_2} \quad (3)$$

RESULTS

Fluorescence Anisotropy of DPH and TMA-DPH in Membranes Containing Cholesterol and Its Immediate Biosynthetic Precursors. The change in fluorescence anisotropy of DPH with increasing sterol concentration is shown in Figure 2. Fluorescence anisotropy is correlated to the rotational diffusion rate (*26*) of membrane-embedded probes,

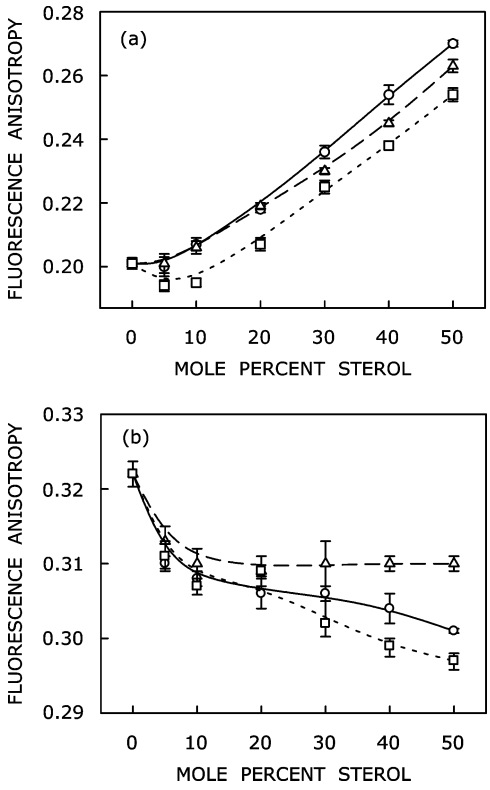

FIGURE 3: Fluorescence anisotropy of TMA-DPH in (a) POPC and (b) DPPC membranes as a function of increasing concentration of cholesterol (○, —), 7-DHC (△, — —), and desmosterol (□, ---). The ratio of TMA-DPH to total lipid was 1:100 (mol/mol), and total lipid concentration was 0.43 mM in all cases. The excitation wavelength used was 358 nm, and emission was monitored at 430 nm. Measurements were carried out at room temperature (~23 °C). Data points shown are the means ± SE of at least three independent measurements. The lines joining the data points are provided merely as viewing guides. See Experimental Procedures for other details.

which is sensitive to the packing of lipid fatty acyl chains and sterols. Figure 2a shows that with increase in cholesterol concentration, DPH anisotropy in fluid POPC membranes shows a continuous increase with a large (~146%) change in anisotropy when 50 mol % cholesterol was incorporated. This could possibly indicate that the membrane becomes more ordered (rigid) with increasing concentration of cholesterol when added to membranes in the fluid phase. This is in agreement with earlier studies in which DPH anisotropy values were reported for POPC (*16*) membranes containing cholesterol.

Although the biophysical characterization of the effect of cholesterol on membranes is well documented by the use of DPH fluorescence (*16*), the effect of immediate precursors of cholesterol in its biosynthetic pathway (such as 7-DHC and desmosterol) on the organization and dynamics of membranes has not been studied in detail, especially using fluorescent membrane probes. The increase in fluorescence anisotropy of DPH in POPC membranes is less (~121%) when 7-DHC was used as the sterol component (Figure 2a). In contrast to this, the increase in DPH fluorescence anisotropy in the case of desmosterol (~144%) was similar to what was observed in the case of cholesterol. The effects of 7-DHC and desmosterol therefore appear to be different on the dynamics (order) of fluid phase POPC membranes, in spite of the fact that both of these sterols differ with cholesterol only in a double bond. It is important to note here that the anisotropy values determined remained identical even after the dilution of membrane samples indicating the absence of any scattering artifacts (*30*).

Figure 2b shows the corresponding changes in DPH anisotropy when sterols were incorporated in the gel phase DPPC membranes at room temperature (~23 °C). Since the fatty acyl chains in DPPC are saturated, it represents a relevant system, as the interaction between saturated fatty acyl chains and sterols has been implicated in raft-type domains. In DPPC membranes containing increasing amounts of cholesterol, the anisotropy value shows a small (~8%) decrease up to 50 mol % cholesterol. This is in agreement with previous results in which it was shown that incorporation of cholesterol makes the gel phase DPPC membranes somewhat less ordered (*16*). In contrast to what was observed in the case of cholesterol containing DPPC membranes, the fluorescence anisotropy of DPH in DPPC membranes exhibits a reduction (~5%) only up to 20 mol % when 7-DHC was used as the sterol component (Figure 2b). At higher concentrations of 7-DHC, the anisotropy values stabilize with increasing 7-DHC concentrations up to 50 mol %. However, the anisotropy value shows a decrease (~9%) when 50 mol % desmosterol was used.

DPH is a rod-like molecule and partitions into the interior of the bilayer. However, its precise location and orientation in the membrane is not known, as DPH does not localize at a unique location in the membrane. In addition, since the membrane is considered as a two-dimensional anisotropic fluid, any possible change in membrane order may not be uniform and restricted to a unique location in the membrane. It is important to monitor the change in membrane order at more than one location in the membrane. We have previously shown that stress such as heat shock can induce anisotropic changes in membrane order, i.e., the change in membrane order was different when monitored in different regions in adult rat liver cell plasma membranes (*31*). Interestingly, such depth-dependent modulation of membrane order induced by alcohols (*32*) and local anesthetics (*33*) has also been reported. We therefore monitored the differential effects of cholesterol and its immediate precursors on membrane dynamics using TMA-DPH. TMA-DPH is a derivative of DPH with a cationic moiety attached to the *para* position of one of the phenyl rings (*34*). While DPH is known to partition into the hydrophobic core of the membrane, the amphipathic TMA-DPH is oriented in the membrane bilayer with its positive charge localized at the lipid−water interface. Its DPH moiety is localized at ~11 Å from the center of the bilayer and reports the interfacial region of the membrane (*35*). In contrast to this, the average location of DPH has been shown to be ~8 Å from the center of the bilayer (*35*).

The change in fluorescence anisotropy of TMA-DPH with increasing sterol concentration is shown in Figure 3. Figure 3a shows that with increase in cholesterol concentration, TMA-DPH anisotropy in fluid POPC membranes shows a continuous increase up to the highest concentration of cholesterol used. There is considerable (~34%) increase in anisotropy when 50 mol % cholesterol was incorporated in POPC membranes. This could possibly indicate that the membrane interfacial region (where the DPH moiety in TMA-DPH is localized) becomes more ordered (rigid) with increasing concentration of cholesterol when added to

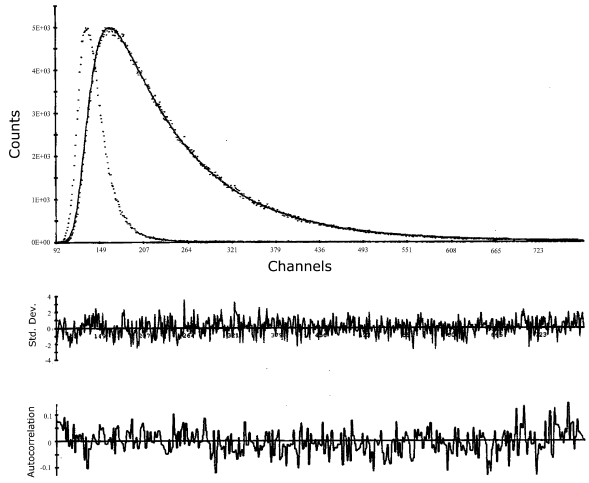

FIGURE 4: Time-resolved fluorescence intensity decay of DPH in DPPC membranes. Excitation wavelength was at 358 nm and emission was monitored at 430 nm. The sharp peak on the left is the lamp profile. The relatively broad peak on the right is the decay profile, fitted to a biexponential function. The two lower plots show the weighted residuals and the autocorrelation function of the weighted residuals. All other conditions are as in Figure 2. See Experimental Procedures for other details.

membranes in the fluid phase. This is consistent with results using DPH in fluid phase POPC membranes (shown in Figure 2a), although the increase in anisotropy of DPH was much higher. The corresponding increase in fluorescence anisotropy of TMA-DPH in POPC membranes is somewhat less (~31%) when 7-DHC was used (Figure 3a). Interestingly, the increase in fluorescence anisotropy of TMA-DPH (~26%) was even less, when desmosterol was used as the sterol component.

The corresponding changes in TMA-DPH anisotropy when sterols were incorporated in the gel phase DPPC membranes at room temperature (~23 °C) are shown in Figure 3b. In DPPC membranes containing increasing amounts of cholesterol, the anisotropy value shows a small (~7%) decrease up to 50 mol % cholesterol. The fluorescence anisotropy of TMA-DPH in DPPC membranes exhibits a reduction (~4%) only up to 20 mol % when 7-DHC was used as the sterol component (Figure 3b). At higher concentrations of 7-DHC, the anisotropy values stabilize with increasing 7-DHC concentrations up to 50 mol %. This suggests that 7-DHC does not influence the membrane order and dynamics in gel phase membranes beyond a certain concentration. When desmosterol was used, the anisotropy value shows a decrease (~8%) up to 50 mol % sterol concentration.

Time-Resolved Fluorescence Measurements of DPH in Membranes Containing Cholesterol and Its Immediate Biosynthetic Precursors. Fluorescence lifetime serves as a faithful indicator of the local environment in which a given fluorophore is placed (*36*). In addition, it is well-known that the fluorescence lifetime of DPH is sensitive to polarity changes in its environment (*37*). All fluorescence decays could be fitted well with a biexponential function. A typical decay profile with its biexponential fitting and the statistical parameters used to check the goodness of the fit is shown in Figure 4. The representative fluorescence lifetimes of DPH in fluid and gel phase membranes, obtained using eq 2, are shown in Tables 1 and 2. The intensity-averaged mean fluorescence lifetimes were calculated using eq 3 and are shown in Figure 5. We chose to use the mean fluorescence lifetime since it is independent of the number of exponentials used to fit the time-resolved fluorescence decay.

Figure 5a shows an increase (~21%) in the mean lifetime of DPH with increasing cholesterol concentration in the fluid

Table 1: Representative Fluorescence Lifetimes of DPH in POPC Membranes in the Presence of Sterols[a]

sterol content (mol %)	α_1	τ_1 (ns)	α_2	τ_2 (ns)
(a) cholesterol				
0	0.75	7.27	0.25	13.63
5	0.69	7.39	0.31	12.66
10	0.66	7.62	0.34	12.75
20	0.61	8.14	0.39	12.68
30	0.49	8.08	0.51	12.26
40	0.76	9.36	0.24	15.58
50	0.89	10.00	0.11	19.44
(b) 7-dehydrocholesterol				
0	0.65	7.02	0.35	12.01
5	0.34	5.98	0.66	10.31
10	0.84	8.02	0.16	16.45
20	0.79	8.01	0.21	15.67
30	0.77	8.20	0.23	16.31
40	0.74	7.98	0.26	15.27
50	0.62	7.83	0.38	14.13
(c) desmosterol				
0	0.38	6.23	0.62	10.76
5	0.50	7.05	0.50	11.87
10	0.31	6.44	0.69	10.95
20	0.79	8.79	0.21	14.51
30	0.56	8.48	0.44	13.10
40	0.68	9.23	0.32	14.60
50	0.63	9.43	0.37	14.04

[a] The excitation wavelength was 358 nm, and emission was monitored at 430 nm in all cases. Concentration of total lipid was 0.43 mM, and the ratio of DPH to total lipid was 1:100 (mol/mol). See Experimental Procedures for other details.

Table 2: Representative Fluorescence Lifetimes of DPH in DPPC Membranes in the Presence of Sterols[a]

sterol content (mol %)	α_1	τ_1 (ns)	α_2	τ_2 (ns)
(a) cholesterol				
0	0.45	8.42	0.55	13.73
5	0.47	8.33	0.53	13.94
10	0.66	9.15	0.34	14.97
20	0.55	8.83	0.45	14.47
30	0.79	9.49	0.21	18.08
40	0.87	9.51	0.13	19.83
50	0.82	9.52	0.18	17.87
(b) 7-dehydrocholesterol				
0	0.55	8.96	0.45	14.13
5	0.24	6.05	0.76	12.12
10	0.21	5.35	0.79	11.42
20	0.27	5.15	0.73	11.44
30	0.27	5.89	0.73	11.77
40	0.21	4.85	0.79	11.00
50	0.27	4.60	0.73	10.49
(c) desmosterol				
0	0.24	7.50	0.76	12.43
5	0.60	9.58	0.40	14.22
10	0.47	8.88	0.53	13.25
20	0.36	8.37	0.64	12.75
30	0.77	9.73	0.23	14.52
40	0.64	9.29	0.36	13.62
50	0.67	9.44	0.33	14.41

[a] The excitation wavelength was 358 nm, and emission was monitored at 430 nm in all cases. Concentration of total lipid was 0.43 mM, and the ratio of DPH to total lipid was 1:100 (mol/mol). See Experimental Procedures for other details.

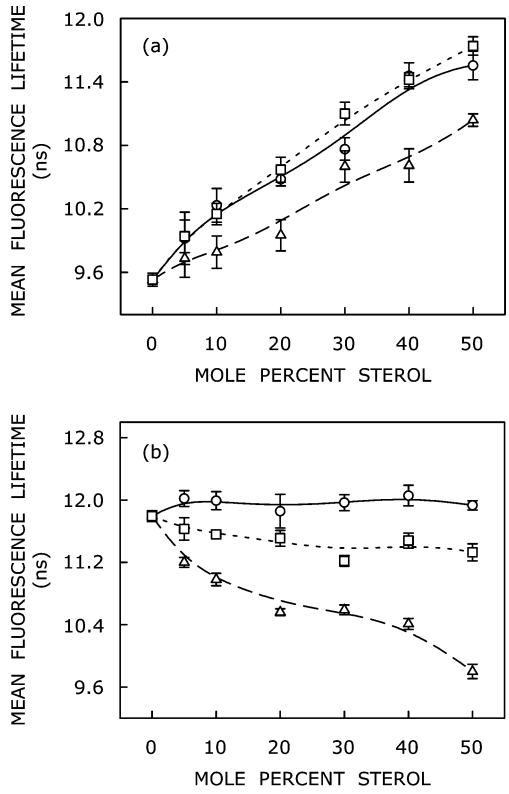

FIGURE 5: Mean fluorescence lifetimes of DPH in (a) POPC and (b) DPPC membranes as a function of increasing concentration of cholesterol (○, —), 7-DHC (△, — —), and desmosterol (□, ---). Mean fluorescence lifetimes were calculated using eq 3. All other conditions are as in Figure 2. Data points shown are the means ± SE of at least three independent measurements. The lines joining the data points are provided merely as viewing guides. See Experimental Procedures for other details.

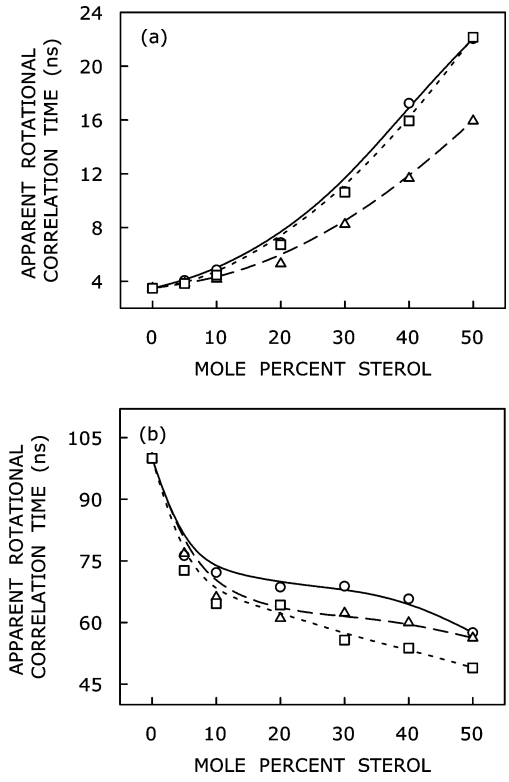

FIGURE 6: Apparent rotational correlation times of DPH in (a) POPC and (b) DPPC membranes as a function of increasing concentration of cholesterol (○, —), 7-DHC (△,— —), and desmosterol (□, ---). Apparent rotational correlation times were calculated from fluorescence anisotropy values of DPH from Figure 2 and mean fluorescence lifetimes from Figure 5 using eq 4. The lines joining the data points are provided merely as viewing guides. See text for other details.

phase POPC membranes. Since DPH lifetime is known to be reduced by the presence of water in its immediate environment (*37, 38*), we interpret the increase in DPH lifetime with increasing cholesterol due to a decrease in water penetration in the bilayer (*39*) because of the rigidification of the fluid membrane upon cholesterol incorporation (Figure 2a). Figure 5a shows that the corresponding increase in DPH lifetime due to the incorporation of increasing concentrations of 7-DHC in the membrane is considerably less (~16%). This may indicate that water penetration is more in the case of 7-DHC, possibly due to the relatively less rigidifying effect of 7-DHC in POPC membranes as previously shown by change in fluorescence anisotropy (Figure 2a). The extent of increase in the mean lifetime of DPH in the case of desmosterol is similar (~23%) to what was observed in the case of cholesterol. The mean fluorescence lifetime of DPH in the gel phase DPPC membranes (~11.8 ns) is considerably higher than what was observed in fluid phase POPC membranes (~9.5 ns), indicating the reduction in polarity experienced by the fluorophore in gel phase, possibly due to decreased water penetration. The effect of increasing concentration of cholesterol on the mean fluorescence lifetime of DPH in gel phase DPPC membranes appears to be minimal (~1% decrease). The mean fluorescence lifetime exhibits a very small decrease (~4%) in the case of desmosterol (see Figure 5b). In contrast, the corresponding reduction in the mean lifetime of DPH is considerably larger (~17%) when 7-DHC was used as the sterol component.

In order to ensure that the anisotropy values measured for DPH (Figure 2) are not influenced by lifetime-induced artifacts, the apparent (average) rotational correlation times were calculated using Perrin's equation (*26*):

$$\tau_c = \frac{\langle \tau \rangle r}{r_o - r} \quad (4)$$

where r_o is the limiting anisotropy of DPH, r is the steady state anisotropy, and $\langle \tau \rangle$ is the mean fluorescence lifetime taken from Figure 5. Although Perrin's equation is not strictly applicable to this system, it is assumed that this equation will apply to a first approximation, especially because we have used mean fluorescence lifetimes for the analysis of multiple component lifetimes. The values of the apparent rotational correlation times, calculated this way using a value of r_o of 0.36 (*40*), are shown in Figure 6. As is evident from the figure, the apparent rotational correlation times show more or less similar trends with increasing sterol concentration as seen in Figure 2. This shows that the observed changes in anisotropy values are largely free from lifetime-induced artifacts.

Environment and Dynamics Experienced by the Hydrophobic Probe Pyrene in Membranes Containing Cholesterol and Its Immediate Biosynthetic Precursors. The fluorescence emission spectrum of pyrene is sensitive to environmental polarity (*41*). Pyrene also forms excimers with very different fluorescence characteristics, and the ratio of excimer/monomer is known to be dependent on membrane dynamics (*42, 43*). Figure 7 shows the fluorescence emission spectra

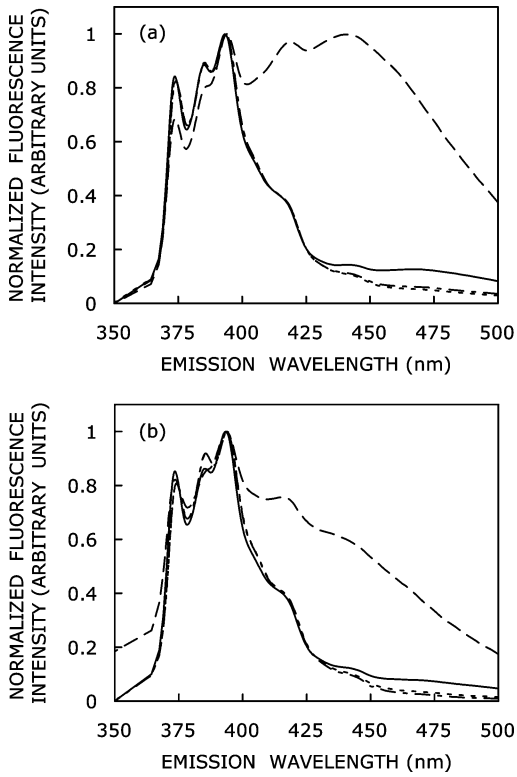

FIGURE 7: (a) Fluorescence emission spectra of pyrene in POPC membranes containing no sterol (—), 50 mol % cholesterol (---), 50 mol % 7-DHC (— —), and 50 mol % desmosterol (— - —). (b) Fluorescence emission spectra of pyrene in DPPC membranes containing no sterol (—), 50 mol % cholesterol (---), 50 mol % 7-DHC (— —), and 50 mol % desmosterol (— - —). The spectra are intensity-normalized at the respective emission maxima. Measurements were carried out at room temperature (~23 °C). The excitation wavelength used was 335 nm. The ratio of pyrene to total lipid was 1:100 (mol/mol), and total lipid concentration was 0.43 mM in all cases. See Experimental Procedures for other details.

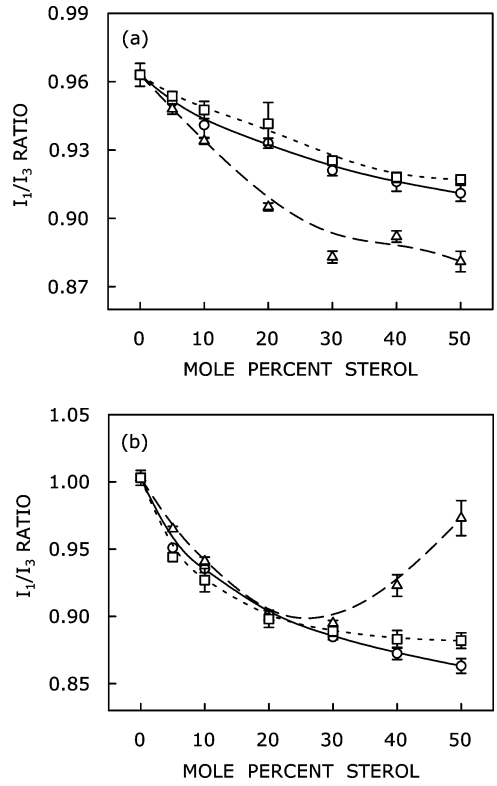

FIGURE 8: Change in the ratio of the first (373 nm) and third (384 nm) vibronic peak intensities of pyrene (I_1/I_3) in (a) POPC and (b) DPPC membranes as a function of increasing concentration of cholesterol (○, —), 7-DHC (△, — —), and desmosterol (□, ---). Data points shown are the means ± SE of at least three independent measurements. All other conditions are as in Figure 7. The lines joining the data points are provided merely as viewing guides. See Experimental Procedures for other details.

of pyrene in the fluid phase POPC and gel phase DPPC membranes and also in the presence of sterols. A characteristic feature of the structured emission spectra is the maxima at 373, 384, and 393 nm. This type of structured vibronic band intensities, displayed by fluorophores, such as pyrene and dehydroergosterol (*44*), are known to be environmentally sensitive. This property has previously been effectively used for elucidating the microenvironments of pyrene (*43, 45*). The ratio of the first (373 nm) and third (384 nm) vibronic peak intensities (I_1/I_3) in the pyrene emission spectrum provides a measure of the apparent polarity of the environment. A reduction in the I_1/I_3 ratio is indicative of decreased polarity. The change in the ratio of vibronic peak intensities (I_1/I_3) in pyrene emission spectra in fluid phase POPC membranes with increasing sterol concentration is shown in Figure 8a. Increasing sterol concentration in general resulted in a decrease in the peak intensity ratio, which could imply a reduction in apparent polarity experienced by pyrene. The reduction in polarity experienced by pyrene could possibly be due to a reduction in water penetration in the bilayer as a result of the rigidification of the fluid membrane upon sterol incorporation (Figure 2a). The decrease in the peak intensity ratio with increasing concentrations of sterol used is similar for membranes containing cholesterol and desmosterol. Interestingly, the reduction in the peak intensity ratio with increasing sterol concentration appears to be sharper when 7-DHC was used, particularly toward higher concentrations. This is somewhat surprising if the reduction in water penetration as a result of the bilayer rigidification would be the sole reason for the decrease in polarity experienced by pyrene. However, the apparent polarity experienced by pyrene could also be influenced by the presence of double bonds, particularly in the shallow region of the bilayer. This is due to the fact that pyrene has been recently reported to be predominantly localized in the interfacial region of the membrane (*46*). The additional double bond at 7th position in 7-DHC is in ring B and therefore localized at a shallow position (an area of the membrane more likely to be sampled by pyrene due to its interfacial localization). This is in contrast to the additional double bond in desmosterol (at 24th position), which is at the flexible alkyl chain region of the molecule and localized deep into the hydrophobic interior of the membrane. This means that the polarity experienced by the interfacial probe pyrene in the case of membranes containing 7-DHC would be considerably influenced by the presence of the additional double bond in the shallow region of the membrane, thereby resulting in reduced peak intensity ratio. Figure 8b shows the corresponding changes in the ratio of pyrene vibronic peak intensities when sterols were incorporated in gel phase DPPC membranes. Interestingly, incorporation of all sterols in gel phase DPPC membranes led to an almost identical reduction in the peak intensity ratio up to 20 mol %. Beyond this point, there is a considerable increase in I_1/I_3 ratio at higher concentrations of 7-DHC, while increasing concentra-

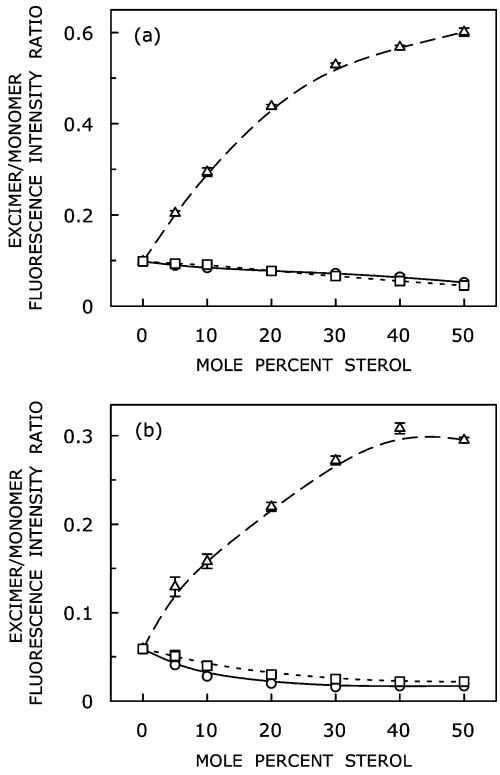

FIGURE 9: Pyrene excimer (480 nm)/monomer (393 nm) fluorescence intensity ratio in (a) POPC and (b) DPPC membranes as a function of increasing concentration of cholesterol (○, —), 7-DHC (△, — —), and desmosterol (□, ---). Data points shown are the means ± SE of at least three independent measurements. All other conditions are as in Figure 7. The lines joining the data points are provided merely as viewing guides. See Experimental Procedures for other details.

tions of cholesterol and desmosterol led to an additional slight reduction in the peak intensity ratio (see Figure 8b).

Another commonly used parameter related to pyrene fluorescence is the excimer/monomer fluorescence intensity ratio (*42, 43*). This parameter is indicative of the extent of pyrene excimerization, which is believed to depend on the monomer lateral distribution and dynamics (diffusion) in the membrane. Nonetheless, the exact mechanism of excimerization is not clear (*47*). Lateral diffusion in membranes is often described in terms of the free volume model (*48, 49*). The free volume framework is a semiempirical approach based on statistical mechanical considerations of density fluctuations in the lipid bilayer. According to this model, transient voids that are created in the lipid bilayer by such density fluctuations are filled by the movement of neighboring lipid molecules into the void. It is generally agreed that the greater the free volume available for pyrene, the higher the level of excimer formation (*43*).

Figure 9a shows the excimer/monomer ratio in fluid phase POPC membranes with increasing sterol concentration. There appears to be a marked difference in the extent of excimer formation with increasing concentrations of cholesterol/desmosterol and 7-DHC. The excimer/monomer ratio shows a small, gradual reduction in the case of cholesterol/desmosterol. Even in gel phase DPPC membranes, the excimer/monomer ratio shows an increase in the case of 7-DHC and decrease in the case of cholesterol/desmosterol. Assuming the excimer/monomer ratio to be indicative of free volume in the membrane bilayer (*43*), 7-DHC appears to increase the free volume with increasing concentration in fluid POPC bilayers. In contrast to this, cholesterol and desmosterol appear to reduce the free volume slightly. Although the change in excimer/monomer ratio in gel phase membranes (see Figure 9b) is similar to what was observed in fluid phase membranes (Figure 9a), the interpretation of the change in excimer/monomer ratio in gel phase is difficult. This is due to the fact that diffusion in the gel phase is known to be influenced by submicroscopic linear defects formed at the interstices of relatively homogeneous gel phase regions of the membrane (*48, 50*). The regions of defects are characterized by greater disorder and enhanced diffusion rates.

DISCUSSION

The overall goal of this work is to explore the effect of cholesterol and its two immediate biosynthetic precursors (7-DHC and desmosterol) on organization and dynamics of fluid and gel phase membranes. For this, we have utilized the fluorescent membrane probes, DPH and TMA-DPH, and the hydrophobic probe, pyrene. While fluorescence anisotropy of probes such as DPH provides information on rotational dynamics in the local (short-range) scale, measurements using pyrene offer more long-range information. Taken together, our results show that the effect of cholesterol and desmosterol on membrane organization and dynamics is similar in most cases, while 7-DHC has a markedly different effect on membrane organization and dynamics. This is an interesting result since both desmosterol and 7-DHC differ only in a double bond with cholesterol. This shows that the position of the double bond is crucial in determining the suitability of sterols in maintaining membrane order and dynamics.

Our results on the similarity in effect of cholesterol and desmosterol on membrane organization and dynamics are in agreement with a previous report in which it was shown that the biophysical properties of desmosterol closely mimic that of cholesterol (*51*). By utilizing NMR, ESR, and laurdan fluorescence spectroscopic approaches, these authors reported that properties such as lipid packing are very similar in the presence of cholesterol and desmosterol. Our present results show that cholesterol and desmosterol share common characteristics in terms of lipid packing at various regions (depths) and long-range diffusion (pyrene excimer/monomer measurements). As mentioned earlier, monitoring lipid dynamics at various locations along the bilayer normal is relevant since sterols are known to influence lipid dynamics in a location-specific manner (*51*). More importantly, our results show that the influence of 7-DHC, an immediate precursor of cholesterol in the Kandutsch-Russell pathway and differing in a double bond, on membrane dynamic properties is considerably different from what is observed with cholesterol and desmosterol. This is supported by results from monolayer studies showing that the packing of 7-DHC is different from the packing of cholesterol and desmosterol in DPPC monolayers (*52*).

Interestingly, it has been recently reported using atomistic simulations that cholesterol and desmosterol differ in their tilt angles with desmosterol having a larger tilt angle (*53*). It is believed that the tilt angle is a measure of the ordering capability of sterols in membranes (the lower the tilt angle,

the higher the ordering ability). On such a basis, it has been suggested that desmosterol will be less efficient in forming raft type of domains. A similar conclusion has recently been derived using approaches based on fluorescence quenching (*54*). This study also reported that the ability of 7-DHC to form raft-like domains is higher than that of cholesterol. As mentioned earlier, the position of the additional double bond appears to be important in the ability to form raft-like domains.

These results assume relevance since accumulation of cholesterol precursors have been reported to result in severe (sometimes fatal) diseases. For example, the accumulation of 7-DHC results in a neurological disorder, namely, the Smith−Lemli−Opitz Syndrome (SLOS) (*55*). SLOS is a congenital and developmental malformation syndrome associated with defective cholesterol biosynthesis. SLOS is caused by mutations in the gene encoding 7-DHCR, an enzyme required in the final step of Kandutsch-Russell pathway of cholesterol biosynthesis. SLOS is clinically diagnosed by reduced plasma levels of cholesterol along with elevated levels of 7-DHC (*10, 55*). However, accumulation of desmosterol results in desmosterolosis (*56*) and is caused by mutations in the gene encoding 24-DHCR, an enzyme required in the ultimate step of the Bloch pathway of cholesterol biosynthesis. Desmosterolosis is clinically characterized by the elevated levels of desmosterol accompanied by the reduced level of cholesterol (*57*).

Comparative studies of the effects of cholesterol and its biosynthetic precursors on membrane properties are significant in the context of the pathogenicity that results because of the deregulation of the biosynthetic pathway. Monitoring the effects on membrane physical properties under these conditions constitute a necessary step to understand the molecular basis of such pathogenicity. Our results show that the effect of cholesterol and desmosterol on membrane organization and dynamics is similar, while 7-DHC has a considerably different effect on membrane organization and dynamics, although both desmosterol and 7-DHC differ with cholesterol only in a double bond. The fine tuning of the structure–function relationship in sterols constitutes a challenging problem and could be useful in understanding the molecular basis of diseases caused by altered sterol biosynthesis.

ACKNOWLEDGMENT

We gratefully acknowledge Ajuna Arora and Sourav Haldar for helpful discussions and Dr. Probal Banerjee (College of Staten Island, City University of New York) for the generous gift of desmosterol during initial experiments. We thank Lora B. Narayana, G. G. Kingi, M. R. V. S. Murty for technical help, and members of our laboratory for critically reading the manuscript.

REFERENCES

1. Schroeder, F., Woodford, J. K., Kavecansky, J., Wood, W. G., and Joiner, C. (1995) Cholesterol domains in biological membranes. *Mol. Membr. Biol. 12*, 113–119.
2. Mouritsen, O. G., and Zuckermann, M. J. (2004) What's so special about cholesterol? *Lipids 39*, 1101–1113.
3. Mukherjee, S., and Maxfield, F. R. (2004) Membrane domains. *Annu. Rev. Cell Dev. Biol. 20*, 839–866.
4. Simons, K., and Ikonen, E. (1997) Functional rafts in cell membranes. *Nature 387*, 569–572.
5. Simons, K., and Toomre, D. (2000) Lipid rafts and signal transduction. *Nat. Rev. Mol. Cell Biol. 1*, 31–39.
6. Pucadyil, T. J., and Chattopahyay, A. (2007) Cholesterol: a potential therapeutic target in *Leishmania* infection? *Trends Parasitol. 23*, 49–53.
7. Kandutsch, A. A., and Russell, A. E. (1960) Preputial gland tumor sterols. III. A metabolic pathway from lanosterol to cholesterol. *J. Biol. Chem. 235*, 2256–2261.
8. Bloch, K. E. (1983) Sterol structure and membrane function. *CRC Crit. Rev. Biochem. 14*, 47–92.
9. Waterham, H. R. (2006) Defects of cholesterol biosynthesis. *FEBS Lett. 580*, 5442–5449.
10. Chattopadhyay, A., and Paila, Y. D. (2007) Lipid-protein interactions, regulation and dysfunction of brain cholesterol. *Biochem. Biophys. Res. Commun. 354*, 627–633.
11. Wechsler, A., Brafman, A., Shafir, M., Heverin, M., Gottlieb, H., Damari, G., Gozlan-Kelner, S., Spivak, I., Moshkin, O., Fridman, E., Becker, Y., Skaliter, R., Einat, P., Faerman, A., Björkhem, I., and Feinstein, E. (2003) Generation of viable cholesterol-free mice. *Science 302*, 3087.
12. Ranadive, G. N., and Lala, A. K. (1987) Sterol-phospholipid interaction in model membranes: Role of C_5-C_6 double bond in cholesterol. *Biochemistry 26*, 2426–2431.
13. Kumari, S. N., Ranadive, G. N., and Lala, A. K. (1982) Growth of a yeast mutant on ring A modified cholesterol derivatives. *Biochim. Biophys. Acta 692*, 441–446.
14. Róg, T., Pasenkiewicz-Gierula, M., Vattulainen, I., and Karttunen, M. (2007) What happens if cholesterol is made smoother: importance of methyl substituents in cholesterol ring structure on phosphocholine-sterol interaction. *Biophys. J. 92*, 3346–3357.
15. Pöyry, S., Róg, T., Karttunen, M., and Vattulainen, I. (2008) Significance of cholesterol methyl groups. *J. Phy. Chem. B. 112*, 2922–2929.
16. Arora, A., Raghuraman, H., and Chattopadhyay, A. (2004) Influence of cholesterol and ergosterol on membrane dynamics: a fluorescence approach. *Biochem. Biophys. Res. Commun. 318*, 920–926.
17. Hsueh, Y. W., Chen, M. T., Patty, P. J., Code, C., Cheng, J., Frisken, B. J., Zuckermann, M., and Thewalt, J. (2007) Ergosterol in POPC membranes: physical properties and comparison with structurally similar sterols. *Biophys. J. 92*, 1606–1615.
18. Samuli Ollila, O. H., Róg, T., Karttunen, M., and Vattulainen, I. (2007) Role of sterol type on lateral pressure profiles of lipid membranes affecting membrane protein functionality: comparison between cholesterol, desmosterol, 7-dehydrocholesterol and ketosterol. *J. Struct. Biol. 159*, 311–323.
19. Vainio, S., Jansen, M., Koivusalo, M., Róg, T., Karttunen, M., Vattulainen, I., and Ikonen, E. (2006) Significance of sterol structural specificity. Desmosterol cannot replace cholesterol in lipid rafts. *J. Biol. Chem. 281*, 348–355.
20. Singh, P., Paila, Y. D., and Chattopadhyay, A. (2007) Differential effects of cholesterol and 7-dehydrocholesterol on the ligand binding activity of the hippocampal serotonin$_{1A}$ receptor: implications in SLOS. *Biochem. Biophys. Res. Commun. 358*, 495–499.
21. Romanenko, V. G., Rothblat, G. H., and Levitan, I. (2002) Modulation of endothelial inward-rectifier K^+ current by optical isomers of cholesterol. *Biophys. J. 83*, 3211–3222.
22. Dittmer, J. C., and Lester, R. L. (1964) Simple, specific spray for the detection of phospholipids on the thin-layer chromatograms. *J. Lipid Res. 5*, 126–127.
23. McClare, C. W. F. (1971) An accurate and convenient organic phosphorus assay. *Anal. Biochem. 39*, 527–530.
24. MacDonald, R. C., MacDonald, R. I., Menco, B. P., Takeshita, K., Subbarao, N. K., and Hu, L. R. (1991) Small-volume extrusion apparatus for preparation of large, unilamellar vesicles. *Biochim. Biophys. Acta 1061*, 297–303.
25. Chattopadhyay, A., and London, E. (1984) Fluorimetric determination of critical micelle concentration avoiding interference from detergent charge. *Anal. Biochem. 139*, 408–412.
26. Lakowicz, J. R. (2006) *Principles of Fluorescence Spectroscopy*, 3rd ed., Springer, New York.
27. O'Connor, D. V., and Philips, D. (1984) *Time-Correlated Single Photon Counting*, pp 180–189, Academic Press, London.
28. Lampert, R. A., Chewter, L. A., Phillips, D., O'Connor, D. V., Roberts, A. J., and Meech, S. R. (1983) Standards for nanosecond fluorescence decay measurements. *Anal. Chem. 55*, 68–73.
29. Grinvald, A., and Steinberg, I. Z. (1974) On the analysis of fluorescence decay kinetics by the method of least-squares. *Anal. Biochem. 59*, 583–598.

30. Lentz, B. R., Moore, B. M., and Barrow, D. A. (1979) Light-scattering effects in the measurement of membrane microviscosity with diphenylhexatriene. *Biophys. J. 25*, 489–494.
31. Revathi, C. J., Chattopadhyay, A., and Srinivas, U. K. (1994) Change in membrane organization induced by heat shock. *Biochem. Mol. Biol. Int. 32*, 941–950.
32. Kitagawa, S., and Hirata, H. (1992) Effects of alcohols on fluorescence anisotropies of diphenylhexatriene and its derivatives in bovine blood platelets: relationships of the depth-dependent change in membrane fluidity by alcohols with their effects on platelet aggregation and adenylate cyclase activity. *Biochim. Biophys. Acta 1112*, 14–18.
33. Yun, I., Cho, E.-S., Jang, H.-O., Kim, U.-K., Choi, C.-H., Chung, I.-K., Kim, I.-S., and Wood, W. G. (2002) Amphiphilic effects of local anesthetics on rotational mobility in neuronal and model membranes. *Biochim. Biophys. Acta 1564*, 123–132.
34. Prendergast, F. G., Haugland, R. P., and Callahan, P. J. (1981) 1-[4-(Trimethylamino)phenyl]-6-phenylhexa-1,3,5-triene: synthesis, fluorescence properties, and use as a fluorescence probe of lipid bilayers. *Biochemistry 20*, 7333–7338.
35. Kaiser, R. D., and London, E. (1998) Location of diphenylhexatriene (DPH) and its derivatives within membranes: comparison of different fluorescence quenching analyses of membrane depth. *Biochemistry 37*, 8180–8190.
36. Prendergast, F. G. (1991) Time-resolved fluorescence techniques: methods and applications in biology. *Curr. Opin. Struct. Biol. 1*, 1054–1059.
37. Stubbs, C. D., Ho, C., and Slater, S. J. (1995) Fluorescence techniques for probing water penetration into lipid bilayers. *J. Fluoresc. 5*, 19–28.
38. Ho, C., and Stubbs, C. D. (1992) Hydration at the membrane protein-lipid interface. *Biophys. J. 63*, 897–902.
39. Subczynski, W. K., Wisniewska, A., Yin, J.-J., Hyde, J. S., and Kusumi, A. (1994) Hydrophobic barriers of lipid bilayer membranes formed by reduction of water penetration by alkyl chain unsaturation and cholesterol. *Biochemistry 33*, 7671–7681.
40. Shinitzky, M., and Barenholz, Y. (1974) Dynamics of the hydrocarbon layer in liposomes of Lecithin and sphingomyelin containing dicetylphosphate. *J. Biol. Chem. 249*, 2652–2657.
41. Dong, D. C., and Winnik, M. A. (1982) The *Py* scale of solvent polarities. Solvent effects on the vibronic fine structure of pyrene fluorescence and empirical correlations with E_T and *Y* values. *Photochem. Photobiol. 35*, 17–21.
42. Vanderkooi, J. M., and Callis, J. B. (1974) Pyrene: a probe of lateral diffusion in the hydrophobic region of membranes. *Biochemistry 3*, 4000–4006.
43. Ioffe, V., and Gorbenko, G. P. (2005) Lysozyme effect on structural state of model membranes as revealed by pyrene excimerization studies. *Biophys. Chem. 114*, 199–204.
44. Rukmini, R., Rawat, S. S., Biswas, S. C., and Chattopadhyay, A. (2001) Cholesterol organization in membranes at low concentrations: effects of curvature stress and membrane thickness. *Biophys. J. 81*, 2122–2134.
45. Haque, M. E., Ray, S., and Chakrabarti, A. (2000) Polarity estimate of the hydrophobic binding sites in erythroid spectrin: a study by pyrene fluorescence. *J. Fluoresc. 10*, 1–6.
46. Hoff, B., Strandberg, E., Ulrich, A. S., Tieleman, D. P., and Posten, C. (2005) ^{2}H-NMR study and molecular dynamics simulation of the location, alignment, and mobility of pyrene in POPC bilayers. *Biophys. J. 88*, 1818–1827.
47. Blackwell, M. F., Gounaris, K., and Barber, J. (1986) Evidence that pyrene excimer formation in membranes is not diffusion-controlled. *Biochim. Biophys. Acta 858*, 221–234.
48. Balcom, B. J., and Petersen, N. O. (1993) Lateral diffusion in model membranes is independent of the size of the hydrophobic region of molecules. *Biophys. J. 65*, 630–637.
49. Vaz, W. L. C., Clegg, R. M., and Hallmann, D. (1985) Translational diffusion of lipids in liquid crystalline phase phosphatidylcholine multibilayers. A comparison of experiment with theory. *Biochemistry 24*, 781–786.
50. Pucadyil, T. J., Mukherjee, S., and Chattopadhyay, A. (2007) Organization and dynamics of NBD-labeled lipids in membranes analyzed by fluorescence recovery after photobleaching. *J. Phys. Chem. B 111*, 1975–1983.
51. Huster, D., Scheidt, H. A., Arnold, K., Herrmann, A., and Müller, P. (2005) Desmosterol may replace cholesterol in lipid membranes. *Biophys. J. 88*, 1838–1844.
52. Berring, E. E., Borrenpohl, K., Fliesler, S. J., and Serfis, A. B. (2005) A comparison of the behavior of cholesterol and selected derivatives in mixed sterol-phospholipid Langmuir monolayers: a fluorescence microscopy study. *Chem. Phys. Lipids 136*, 1–12.
53. Aittoniemi, J., Róg, T., Niemelä, P., Pasenkiewicz-Gierula, M., Karttunen, M., and Vattulainen, I. (2006) Tilt: major factor in sterols' ordering capability in membranes. *J. Phys. Chem. B 110*, 25562–25564.
54. Megha, Bakht, O., and London, E. (2006) Cholesterol precursors stabilize ordinary and ceramide-rich ordered lipid domains (lipid rafts) to different degrees: Implications for the Bloch hypothesis and sterol biosynthesis disorders. *J. Biol. Chem. 281*, 21903–21913.
55. Waterham, H. R., and Wanders, R. J. A. (2000) Biochemical and genetic aspects of 7-dehydrocholesterol reductase and Smith-Lemli-Opitz syndrome. *Biochim. Biophys. Acta 1529*, 340–356.
56. FitzPatrick, D. R., Keeling, J. W., Evans, M. J., Kan, A. E., Bell, J. E., Porteous, M. E. M., Mills, K., Winter, R. M., and Clayton, P. T. (1998) Clinical phenotype of desmosterolosis. *Am. J. Med. Genet. 75*, 145–152.
57. Herman, G. (2003) Disorders of cholesterol biosynthesis: prototypic metabolic malformation syndromes. *Hum. Mol. Genet. 12*, R75–R88.

BI8001677